high-pressure ratios and vortex shedding (Fig. 3b) at low-pressure ratios with hysteresis for the discharge coefficient (Fig. 2b). The SA turbulence model also gives both flow regimes, but without the hysteresis, and the flow becomes steady again at low-pressure ratios. The k–ε turbulence model does not predict any vortex shedding. Transient boundary conditions were used changing P/p in steps of $0.01 \cdot p$ in the hysteresis region. Almost all simulated values are within the range of the different experimental data sets from Refs. 3 and 4. Note that the measured discharge coefficients from Ref. 3 appear to be overestimated by 4–5% (Ref. 8). The vortex shedding flow regime shows higher discharge coefficients than steady-state flow.

Simulations for incompressible flow were made using pipes with four times the orifice diameter and a finer mesh at $Re = 1.028 \times 10^5$. Vortex shedding is suppressed for a constant mass flow rate by prescribing the velocity at the inlet. The discharge coefficients for the incompressible case (Fig. 2b, $P/p = 1$) match the compressible numerical results well.

A mesh refinement by quadrupling cells for the zero length orifice with RS turbulence model at $P/p = 1.074$ increases the discharge coefficient by 0.5%. Taking a 10 times smaller time step for $l/d = 1/2$ for the RS turbulence model at $P/p = 1.074$ increases the discharge coefficient by less than 1%. In contrast to the zero length orifice, the wide variation of the results for $t/d = 1/2$ for different turbulence models indicates the limitation of the numerical method for modeling this configuration. However, the results of the RS turbulence model seem to replicate the physics of the arrangement qualitatively. They confirm the hysteresis in the discharge coefficient and the vortex whistle mechanism.

Whether the pipe geometry has a significant influence on the discharge coefficient with respect to resonances needs to be examined. However, the vortex shedding for the incompressible simulation, where resonances cannot be taken into account, indicates that this is not the case.

Conclusions

It has been shown that the hysteresis observed previously can be explained by the transition between two flow regimes, which are defined by steady-state flow at high-pressure ratios and vortex shedding at low-pressure ratios. Because the vortex shedding is part of the vortex whistle mechanism, the hysteresis effect is linked to this phenomenon.

The results are consistent with the initial observations, which include a hysteresis, a train of vortex rings, and a vortex whistle. Transitions between the two flow regimes, that is, separated flow and reattached flow, with a hysteresis[2] cannot be confirmed.

Acknowledgments

Simulations have been performed during a placement of the first author at Rolls–Royce, plc. Ansty, England, United Kingdom. The authors thank B. Whinray, D. Livingstone, G. D. Snowsill, J. P. Kunsch, and S. Schlamp for their help and advice.

References

[1]Lichtarowicz, A., Duggins, R. K., and Markland, E., "Discharge Coefficients for Incompressible, Noncavitating Flow Through Long Orifices," *Journal of Mechanical Engineering Science*, Vol. 7, No. 2, 1965, pp. 210–219.

[2]Ward-Smith, A. J., *Pressure Losses in Ducted Flows*, Butterworths, London, 1971, pp. 135–157.

[3]Hay, N., and Spencer, A., "Discharge Coefficients of Cooling Holes with Radiused and Chamfered Inlets," *Journal of Turbomachinery*, Vol. 114, No. 4, 1992, pp. 701–706.

[4]Deckker, B. E. L., and Chang, Y. F., "An Investigation of Steady Compressible Flow Through Thick Orifices," *Thermodynamics and Fluiddynamics Convention 1966*, Vol. 180, Pt. 3J, Institution of Mechanical Engineers, London, 1966, pp. 312–323.

[5]Morse, P. M., and Ingard, K. U., *Theoretical Acoustics*, Princeton Univ. Press, Princeton, NJ, 1968, pp. 755–758.

[6]"FLUENT5 User's Guide," Fluent, Inc., Lebanon, NH, July 1998.

[7]Rayer, Q. G., and Snowsill, G. D., "Validation of FLUENT Against Incompressible and Compressible Flow Through Orifices," *CFD in Fluid Machinery Design*, Professional Engineering Publishing, Bury St. Edmunds, England, U.K., 1998, pp. 79–91.

[8]Parker, D. M., and Kercher, D. M., "An Enhanced Method to Compute the Compressible Discharge Coefficient of Thin and Long Orifices with Inlet Corner Radiusing," *Heat Transfer in Gas Turbine Engines*, Vol. 188, American Society of Mechanical Engineers, New York, 1991, pp. 53–63.

K. N. Ghia
Associate Editor

Low-Temperature Effects on E-Glass/Urethane at High Strain Rates

Shunjun Song* and Jack R. Vinson†
University of Delaware, Newark, Delaware 19716
and
Roger M. Crane‡
U.S. Naval Surface Warfare Center, West Bethesda, Maryland 20817-5700

Introduction

COMPOSITE materials are used in a wide variety of low-temperature applications because of their unique and highly tailorable properties. These low-temperature applications of composites include their use in arctic environments and most of them involve dynamic loads. According to the U.S. Navy, under certain conditions naval vessels may encounter strain rate up to 1200/s. Because the dynamic properties of composite materials may vary widely with strain rate, it is important to use these dynamic properties in design when the loading conditions require it.

All too few materials have been characterized both at high strain rates and at low temperature. Still less effort has been spent in trying to model the high strain rate properties to develop a predictive capability. It has been hoped that earlier modelings for metals, such those as Johnson and Cook[1] and Zerilli and Armstrong[2] might be used for composite materials. The Johnson–Cook model was modified by Weeks and Sun[3] for composite materials. Other recent modeling and research have been performed by Thiruppukuzhi and Sun,[4] Hsiao et al.[5] and Tsai and Sun.[6] Vinson and Woldesenbet[7] have characterized the high strain rate and fiber orientation effects on one typical graphite/epoxy composite. Most of these characterizations model ultimate strengths only.

Over the last several years a program has been conducted to determine experimentally the dynamic compressive material properties of various composite materials that are of interest to industry and to various government agencies. A split Hopkinson pressure bar was used for all of these compression experiments. In all cases, at least three replicate specimens were tested, and subsequently the data was analyzed to determine both mean values and standard deviations. Those experiments were conducted at room temperature, and the results are presented in Refs. 8–18. The mean values of those data[8–18] were presented recently in Ref. 19, where polynomial expressions for the ultimate strengths and moduli of elasticity were

Received 17 July 2002; revision received 14 October 2003; accepted for publication 3 November 2003.

*Research Assistant, Department of Mechanical Engineering; currently Ph.D. Candidate, Department of Aerospace Engineering, University of Michigan, Ann Arbor, MI 48109. Student Member AIAA.

†H. Fletcher Brown Professor, Department of Mechanical and Aerospace Engineering; vinson@me.udel.edu. Fellow AIAA.

‡Composite Materials Section Head, Carderock Division.

developed for the materials tested over the range of strain rates that were investigated.

This study extends the experiments at high strain rate compressive testing from room temperature down to the liquid nitrogen temperature (−196°C). The same equipment, testing technique, and data reduction were employed for these tests as were used for the previous room temperature tests.

Standard Equipment

The split Hopkinson pressure bar is used to obtain high strain rate compressive properties of the tested materials. It is an inexpensive device for performing high strain rate experiments. This apparatus consists of three long pressure bars, that is, striker bar, incident bar, and transmission bar. The specimen is sandwiched between the transmission and incident bar. A striker bar is propelled by nitrogen gas released from a tank, strikes the incident bar, sending a compressive wave into the incident bar. Strain gauges are mounted on the incident and transmission bars equidistant from the specimen interfaces and are connected to an oscilloscope. The oscilloscope records and keeps all of the output from the strain gauges. When it is assumed that wave propagation in the bars is nondispersive, the force and displacement at the contact between the bar and specimen can be derived from the measured strains, and further, the strain rate, ultimate strength, and ultimate strain can also be derived using well-known equations. Usually, the range of the strain rates varies from 250 to 2000/s.

Modified Equipment

To perform high strain rate tests under low temperature, the following changes are made to the split Hopkinson pressure bar (SHPB) device. A low-temperature dewar supported by a laboratory stand is used to drip liquid nitrogen down to the specimen, which is sandwiched between the incident and transmission bars. The specimen was soaked in a liquid nitrogen bath for over 1 h before being placed in the SHPB device. The specimen temperature is monitored by the thermocouple temperature monitor, where the up-to-the-second temperature can be read, so that any predetermined temperature can be chosen to be the testing temperature. This continues until the specimen reaches a uniform temperature throughout its volume.

Specimen Description and Testing Conditions

An E-glass/urethane material is tested in this study, and the specimens were provided by the U.S. Naval Surface Warfare Center, at Carderock, Maryland. They are small cubes measuring 6.25 mm on each edge with the three directions x, y, and z marked on each specimen. The cross-ply configuration involves the fibers all being in the x–y plane, whereas z is the through-thickness direction. The fiber volume fraction is 48%.

The specimens are tested in dynamic conditions with strain rates from 1521.3 up to 2005.0 1/s in the x direction, from 1353.0 to 1895.1 1/s in the y direction, and 1713.6 to 1925.1 1/s in the z direction. Along every direction, five temperature points, −196, −100, −50, 0, and 25°C (room temperature), were selected where the tests were performed, but due to difficulty in practice, the actual temperatures were different to some degree, but fairly close. Also, at every temperature point, there were at least three specimens tested so that the mean and deviation can be obtained.

Results and Discussion

From the experiments, most E-glass/urethane specimens fracture into small pieces. Examination of the collected pieces and the scanning electron microscope photographs show that interply delamination is the primary failure mode.

It is found that the effects of low temperature are significant on properties such as ultimate compressive strength, total strain energy density to failure, and the modulus of elasticity. As will be shown the experiments were conducted with a constant nitrogen tank pressure of 0.28 MPa because the focus of these early experiments is to show the effects of temperature primarily, not varying strain rates. Although the nitrogen pressure was held constant, it is seen that strain

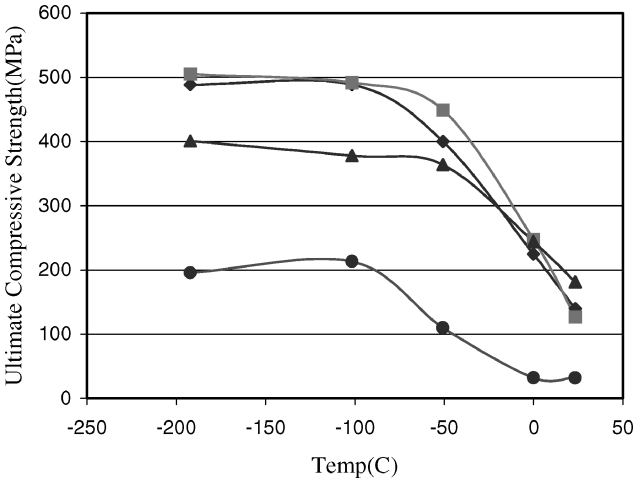

Fig. 1 Comparison of ultimate compressive strength of E-glass/urethane in the *x*, *y*, and *z* directions and pure resin: ◆, *x* direction; ■, *y* direction; ▲, *z* direction; and ●, pure resin.

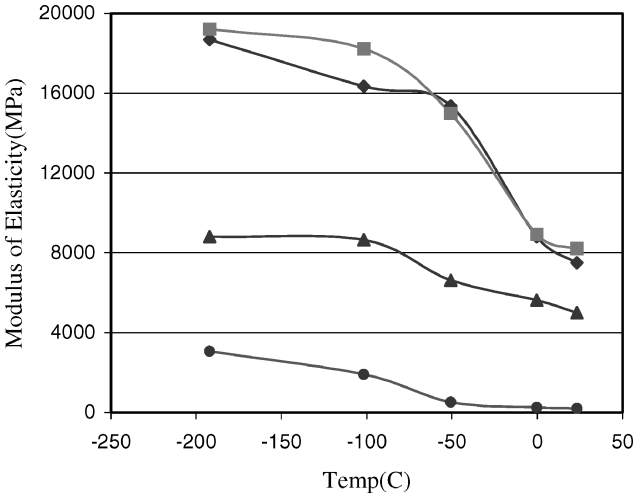

Fig. 2 Comparison of modulus of elasticity of E-glass/urethane in the *x*, *y*, and *z* directions and pure resin: ◆, *x* direction; ■, *y* direction; ▲, *z* direction; and ●, pure resin.

rates do vary somewhat from test to test. As described before, x and y directions are in-plane along which the fibers are aligned, whereas the z direction is the thickness direction, which is matrix dominated and, therefore, comparatively weak. When Figs. 1–3 are examined, one finds that the properties at low temperature are greatly improved compared with those at higher temperatures; for example, in Fig. 2, the moduli in the x and y directions are much larger than those at higher temperature, increasing 2.48 and 2.34 times, respectively. Consequently one hypothesis is proposed: The resin is sensitive to temperature change. When exposed to very low temperature, the resin becomes stiffer, thus better supporting the fibers so that they resist higher stress failure and buckling loads, that is, the fibers are supported on an improved elastic foundation, which increases significantly as the temperature is reduced. Finally, when the matrix fails, interfacial debonding occurs. The hypothesis has been verified by performing the tests of the urethane neat resin at the same temperatures. Clearly in Fig. 1, the ultimate compressive strength of the neat resin increases by a factor of 6 from 32.2 to 195.7 MPa as the temperature goes from 24.9°C down to −192.3°C. Meanwhile the ultimate compressive strength of the composite increases about 3.5 times along the x direction and 4 along the y direction. Also, it can be seen in Fig. 3 that the strain energy density increases more than twice as much from 23.3°C down to −191.2°C. Thus, it can be seen that not only the elastic constants, such as modulus of elasticity, shear modulus, or Poisson's ratio follow some certain

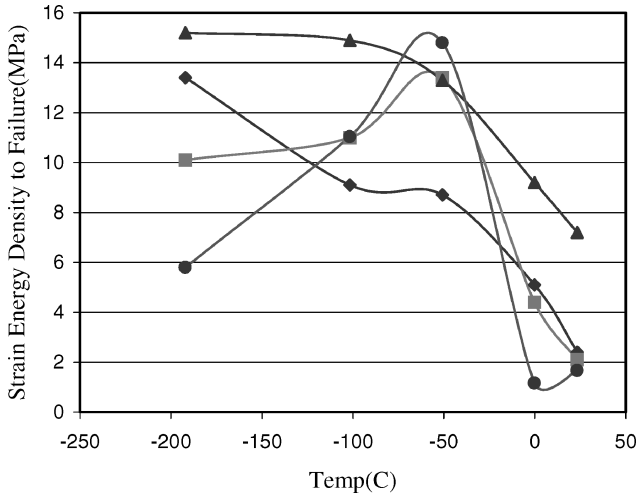

Fig. 3 Comparison of strain energy density to failure of E-glass/urethane in the *x*, *y*, and *z* directions and pure resin: ◆, *x* direction; ■, *y* direction; ▲, *z* direction; and ●, pure resin.

rule, but also all other properties, for example, ultimate strength and strain energy density to failure do so also. The rule is similar to the rule of mixtures $P = (P_f V_f + \eta P_m V_m)/(V_f + \eta V_m)$ derived by Hahn,[20] where P_f and P_m are the properties of the fiber and the matrix to be calculated, respectively, and V_f and V_m refer to the volume fraction of the fiber and the matrix, respectively. Therefore, if a composite material requiring strong properties is to be used, but the fiber is not available, then the matrix can be of use if it is much stronger under cryogenic conditions. In other words, the matrix can be mixed with an other comparatively weaker fiber to still provide desired strong properties. However so far, the data are insufficient. We cannot derive the formula to determine the constant η governing such a phenomenon.

Comparison Among *x*-, *y*- and *z*-Direction Tests

From the preceding analysis, it is easily seen that properties along the *x* and *y* directions, that is, in-plane directions, have much larger increases from room temperature to liquid nitrogen temperature, than those in the *z* direction, the through-thickness direction, which is matrix dominated and, therefore, comparatively weak. Also at the liquid nitrogen temperature point, the ultimate strength values along the in-plane *x* and *y* directions are equal to each other and are greater than the values in the thickness direction. For the modulus of elasticity, the same thing happens, but it seems that strain energy density to failure does not follow these trends. The preceding discussion can be seen in Figs. 1–3.

Before this study, there was very little[21–23] experimental data for high strain rate mechanical properties of composite materials at temperature approaching the liquid nitrogen temperature.

Conclusions

For the E-glass/urethane materials, at a constant strain rate, when various properties in going from room temperature to liquid nitrogen temperature were compared, the following results were obtained. In the *x* direction, 1) the ultimate compressive strength increased 249.3%, 2) the modulus of elasticity increased 148.8%, and 3) the strain energy density to failure increased 458.3%. In the *y* direction, 1) the ultimate compressive strength increased 298.2%, 2) the modulus of elasticity increased 133.8%, and 3) the strain energy density to failure increased 381.0%. In the *z* direction, 1) the ultimate compressive strength increased 121.1%, 2) the modulus of elasticity increased 76.5%, and 3) the strain energy density to failure increased 111.1%. For neat resin, 1) the ultimate compressive strength increased 507.8%, 2) the modulus of elasticity increased 1463.0%, and 3) the strain energy density to failure increased 241.2%.

When the data for the *x*, *y*, and *z* directions are compared, it is seen that changes of ultimate compressive strength, modulus, and strain energy density to failure in the *x* and *y* directions are larger than those in the *z* direction, where *z* is the thickness direction.

Primarily it is the increase in the properties of the neat urethane resin that makes the significant increase of the composite material properties between room temperatures and the reduced temperatures. Also the properties follow the rule of mixtures provided by Hahn.[20]

Acknowledgments

Appreciation is expressed to the Office of Naval Research, which supported this research through Grant N000 14-93-1-1014, and to Yapa D.S.Rajapakse, the Project Manager.

References

[1]Johnson, G. R., and Cook, W. H. "Fracture Characteristics of Three Metals Subjected to Various Strains, Strain Rates, Temperatures and Pressures," *Engineering Fracture Mechanics*, Vol. 21, 1985, pp. 31–48.

[2]Zerilli, F. J., and Armstrong, R. W., "Dislocation Mechanics-Based Constitutive Relations for Material Dynamic Calculations," *Journal of Applied Physics*, Vol. 6, 1987, pp. 1816–1825.

[3]Weeks, C. R., and Sun, C. T., "Nonlinear Rate Dependent Response of Thick-Section Composite Laminates," *High Strain Rate Effects on Polymer, Metal and Ceramic Matrix Composite and Other Advanced Materials*, coedited by Y. D. S. Rajapakse and J. R. Vinson, ASME AD-Vol. 48, American Society of Mechanical Engineers, Fairfield, NJ, 1995, pp. 109–114.

[4]Thiruppukuzhi, S. V., and Sun, C. T., "Testing and Modeling High Strain Rate Behavior of Polymeric Composites," *Composites*, Pt. B, Vol. 29B, 1998, pp. 535–546.

[5]Hsiao, H. M., Daniel, I. M., and Cordes, R. D., "Strain Rate Effects on the Transverse Compressive and Shear Behavior of Unidirectional Composites," *Journal of Composite Materials*, Vol. 33, No. 17, 1999, pp. 1620–1642.

[6]Tsai, J., and Sun, C. T., "Nonlinear Constitutive Model for High Strain Rate Response in Polymeric Composites," *Proceedings of the 15th Annual Technical Conference of the American Society for Composites*, College Station, TX, 2000, pp. 421–430.

[7]Vinson, J. R., and Woldesenbet, E., "Fiber Orientation Effects on High Strain Rate Properties of Graphite/Epoxy Composites," *Journal of Composite Materials*, Vol. 35, No. 6, 2001, pp. 509–522.

[8]Powers, B. M., Vinson, J. R., Hall, I. W., and Hubbard, R. F., "High Strain Rate Mechanical Properties of Cycom 5920/1583," *Proceedings of the 36th AIAA/ASME/ASCE/AHS/ASC Structures, Structural Dynamics, and Materials Conference*, AIAA, Washington, DC, 1995, pp. 2386–2392.

[9]Dee, A. T., and Vinson, J. R., "The Effect of High Strain Rate on the Compressive Mechanical Properties of Unidirectional Glass/Epoxy (3M Scotchply 1003)," *Proceedings of the 12th American Society for Compressive Annual Technical Conference*, Dearborn, MI, 1997, pp. 399–408.

[10]Powers, B. M., and Vinson, J. R., "High Strain Rate Mechanical Properties of IM7/8551-7 Graphite Epoxy," *Proceedings of the 10th American Society for Composites Annual Technical Conference*, Santa Monica, CA, 1995, pp. 227–238.

[11]Dee, A. T., Vinson, J. R., and Leon, G., "High Strain Rate Mechanical Properties of a Torospherical Shell Composed of IM7/E7T1-2 Graphite Epoxy Composite," *11th International Conference on Composite Materials*, American Educational Systems, 1997.

[12]Powers, B. M., Vinson, J. R., Wardle, M., and Scott, B., "High Strain Rate Effects on Two Graphite Fiber K3B Polyimide Matrix Composites," *Proceedings of the 37th AIAA/ASME/ASCE/AHS/ASC Structures, Structural Dynamics, and Materials Conference*, AIAA, Reston, VA, 1996, pp. 30–38.

[13]Powers, B. M., Vinson, J. R., Wardle, M., and Scott, B., "High Strain Rate Effects on Two AS4 Graphite Fiber Polymer Matrix Composites," *High Strain Rate Effects on Polymer, Metal and Ceramic Matrix Composites and Other Advanced Materials*, coedited by Y. D. S. Rajapakse and J. R.Vinson, ASME AD-Vol. 48, American Society of Mechanical Engineers, Fairfield, NJ, 1995, pp. 179–189.

[14]Powers, B. M., Vinson, J. R., Wardle, M., and Scott, B., "High Strain Rate Effects on AS4/PEKK Graphite Fiber Thermoplastic Matrix Composites," *Proceedings of the 11th American Society for Composites Annual Technical Conference*, Atlanta, 1996, pp. 486–494.

[15]Preissner, R. C., Woldesenbet, E., and Vinson, J. R., "High Strain Rate Compression Testing of K49/350-6Kevlar/Epoxy Composites," *Proceedings of the 38th AIAA/ASME/ASCE/AHS/ASC Structures, Structural Dynamics, and Materials Conference*, AIAA, Reston, VA, 1997, pp. 935–944.

[16]Powers, B. M., Vinson, J. R., Hall, I. W., and Nardone, V., "High Strain Rate Mechanical Properties of Silicon Carbide Reinforced 2080 Aluminum Metal Matrix Composites," *Proceedings of the 10th International Conference on Composite Materials*, Vol. 2, 1995, pp. 317–322.

[17]Dee, A. T., Vinson, J. R., and Sankar, B. V., "Effects of High Strain Rate Compression on the Mechanical Properties of a Uniweave A54/3501-6 Composite Laminate with Through-Thickness Stitching," *Proceedings of the 38th AIAA/ASME/ASCE/AHS/ASC Structures, Structural Dynamics, and Materials Conference*, AIAA, Reston, VA, 1997, pp. 945–955.

[18]Greenfield, R., Vinson, J. R., and Telegadas, H., "High Strain Rate Tensile Properties of Woven Glass Fabric Composites," *Proceedings of the 39th AIAA/ASME/ASCE/AHS/ASC Structures, Structural Dynamics, and Materials Conference*, AIAA, Reston, VA, 1998, pp. 1362–1371.

[19]Vinson, J. R., and Xiao, S., "On Predicting the Dynamic Failure in Composite Materials under Compressive and Tensile Loads," American Society of Mechanical Engineers–IMECE, New York, Nov. 2001.

[20]Hahn, H. T., "Simplified Formulas for Elastic Moduli of Unidirectional Continuous Fiber Composites," *Composite Technology Review*, Vol. 2, No. 3, 1980, pp. 5–7.

[21]Song, S., Vinson, J. R., and Crane, R. M., "Low Temperature Effects on E-glass/Urethane Composite Material at High Strain Rates," 43rd AIAA/ASME/ASCE/AHS/ASC Structures, Structural Dynamics, and Materials Conf., April 2002.

[22]Song, S., and Vinson, J. R., "Low Temperature Effects on IM7/977-3 Cross-ply Composite Material Properties at High Strain Rates," American Society of Mechanical Engineers International Mechanical Engineering Congress and Exposition, Nov. 2002.

[23]Song, S., "The Behavior of Several Composite Materials under Both Low Temperatures and High Strain Rates," M.S. Thesis, Dept. of Mechanical Engineering, Univ. of Delaware, Newark, DE, Aug. 2002.

K. N. Shivakumar
Associate Editor